MICHIGAN STATE UNIVERSITY

CYCLOTRON LABORATORY

QUASI-ELASTIC (p,p′) REACTIONS IN SIMPLIFIED RESPONSE MODELS

J. JAENICKE, G. BERTSCH, G. CHANFRAY,
H. ESBENSEN, and P. SCHUCK

JUNE 1990

MSUCL-730

MSUCL-730
June, 1990

Quasi-Elastic (p,p') Reactions in Simplified Response Models

J. JAENICKE (A), G. BERTSCH (B), G. CHANFRAY (D),

H. ESBENSEN (B,E), AND P. SCHUCK (C)

(A) University of Heidelberg, Institut für Theoretische Physik, D-6900 Heidelberg 1, F.R.G.

(B) Physics Department and Cyclotron Laboratory, Michigan State University, East Lansing, MI 48824

(C) Institut des Sciences Nucléaires, F - 38026 Grenoble-Cedex, France

(D) Université C. Bernard Lyon I, F - 69622 Villeurbanne, France

(E) Physics Division, Argonne National Laboratory, Argonne IL 60439

Abstract, Quasi-elastic proton scattering at 290, 400 and 500 MeV bombarding energy is calculated with two simplifed models, the surface response model and the Thomas-Fermi model, and compared with data. Both models describe the data quite well, even though the physical assumptions are somewhat different. The agreement is in fact rather better than previously reported.

1. Introduction

Recently two simplified models of the nuclear response have been put forward, the surface response model of Esbensen and Bertsch [1] and the semiclassical model of Schuck et al.[2]. These models are based on rather different assumptions, and in this paper we wish to compare their predictions. Both models are approximations to the quantal mean field theory (RPA), but they lack the shell structures characteristic of finite potential fields. However, no shell effects are visible in the empirical nuclear response beyond about 20 MeV excitation. Thus these models are attractive since they have no more detail than the data.

In this paper we also examine the comparison with the inelastic scattering data of ref. [3] and [4]. The models have been applied to the data before, but because of flaws in previous comparisons the quantitative validity of the models was not properly assessed. In the case of the Thomas-Fermi model, the normalization was incorrect in ref. [2] due to an error in transforming from center-of-mass to laboratory system. The application of the surface response model in ref. [3,4] omitted the residual interaction, which plays a significant role.

The main features of the models are as follows. The surface response model ignores spherical geometry, but treats the non-locality of the response in detail. The Thomas-Fermi approximation ignores the non-locality of the response and quantum effects associated with the surface. It has been shown, however, in ref. [5] that the neglect of these features introduces only small errors. On the other hand, also the neglect of sphericity in the surface response model is of minor importance. Thus it is not astonishing that both models give quite similar results, the differences may be mostly due to the use of different effective forces. The Thomas-Fermi model is numerically simpler than the surface response model. Qualitatively, both models have an enhanced isoscalar response in the surface region. This is due to two effects: a strong attraction of the residual force at low densities and the translational degeneracy of the surface position (Goldstone mode).

2. Thomas-Fermi approach.

The Thomas-Fermi approximation to the nuclear response has been extensively described in a recent review article and we refer the reader to that for more details of the formalism [2]. This model was first used in ref. [6]; it is also discussed in ref. [1].

The differential cross section is expressed in terms of a Thomas-Fermi response function $\Pi_i^{TF-RPA}(R,q,\omega)$ depending on coordiante R, momentum transfer q, and energy transfer ω as follows.

$$\frac{d\sigma}{d\omega dE} = \sum_i \left(\frac{d\sigma}{d\omega}\right)^{el}_{i,\theta,E_p} \int d^3R\, C(R)\, \frac{-Im\,\Pi_i^{TF-RPA}}{\pi} \tag{1}$$

Here $(d\sigma/d\omega)^{el}$ is the free elastic scattering. For this expression, we used the parameterization of [7] which is based on an analysis of experimental phase shifts. The index i runs over all spin and isospin channels. Explicitly, S and T can take the values of 0 and 1.

The optical cut-off factor $C(R)$ is derived from the eikonal approximation to the DWBA wave functions for the incoming and outgoing protons, using a classical approximation for the imaginary part of the optical potential [8]. It reads

$$C(R) = \frac{1}{2}\int_{-1}^{1} dx\, exp\Big(-\sigma \int_{-\infty}^{\infty} dz\, \rho(\sqrt{R^2(1-x^2)+z^2})\Big). \tag{2}$$

For σ we use here the free nucleon-nucleon cross section of 30 mb.

The polarization operator, Π_i^{TF-RPA}, is calculated in Thomas-Fermi approximation and includes the residual interactions at the level of the Random Phase Approximation (RPA). The detailed expression is given by

$$\Pi_i^{TF-RPA}(R,q,\omega) = \frac{\Pi^{0TF}(R,q,\omega)}{1 - v^i_{eff}(R,q,\omega)\Pi^{0TF}(R,q,\omega)}. \tag{3}$$

with

$$\Pi^{0TF}(R,q,\omega) = 4\int \frac{d^3p}{(2\pi)^3}\Big(\frac{\theta(k_F(R)-p)\theta(|p+q|-k_F(R))}{\omega - H_{p+q} + H_p + i\eta}$$

$$-\frac{\theta(p-k_F(R))\theta(k_F(R)-|p+q|)}{\omega - H_p + H_{p+q} + i\eta}\Big) \tag{4}$$

where $H_p = H(R,p) = p^2/2m + V(R,p)$ is the Wigner transform of the non-local Hartree-Fock Hamiltonian. In practice, the mean-field $V(R,p)$ is calculated self-consistently from the Gogny interaction [9], so no effective mass approximation is introduced. The local Fermi momentum is $k_F(R) = (6\pi^2\rho(R))^{1/3}$.

Sometimes expressions similar to eq.(3,4) are evaluated with a shift added to ω to account for binding effects. This is incorrect, since eq. (3,4) are the strict $\hbar \to 0$ limits of the corresponding quantal expression [2].

Let us explain in more detail the fully antisymmetrized effective interaction, $v^i_{eff}(q)$, of equation (3). The direct and exchange contributions are of the same order of magnitude and it is very important to treat both on the same footing. For finite range forces, to be considered here, the inclusion of exchange leads to a genuine integral equation for the polarization operator, even in infinite matter. There is therefore no analytical solution, even in the local density approximation. For nuclear matter, on the other hand, the polarization propagator can always formally be written as [11]

$$\Pi^{n.m.}(k_F,q,\omega) = \frac{\Pi^{0n.m.}(k_F,q,\omega)}{1 - m(k_F,q,\omega)\Pi^{0n.m.}(k_F,q,\omega)} \tag{5}$$

Now all the difficulties are contained in the unknown function $m(k_F,q,\omega)$. In the ring approximation it reduces to the direct part $v_i(q)$ of the residual interaction. In this approximation, eq. (5) is the exact solution of the RPA equation for infinite matter. Calculating $m(k_F,q,\omega)$ to first order in the interaction

$$m^{(1)}(k_F, q, \omega) = v_{eff}(k_F, q, \omega) \tag{6}$$

leads to our expression (3). This corresponds to the lowest order continued fraction approximation of the polarization propagator including exchange. Introducing this expression in eq. (5) and replacing k_F by $k_F(R)$ gives us the response function, where the exchange contribution of the residual interaction is approximately taken into account. More details are given in ref. [12].

Explicitly, we use for the residual interaction phenomenological nuclear forces, which agree quite well with Brueckner G-Matrix calculations up to momentum transfers of the order of the Fermi momentum. For the spin independent channels, we take Gogny's interaction which has already succesfully been employed in our previous nuclear response calculations [10,11]. It is well-known that this force reproduces quite accurately a number of nuclear quantities in addition to ground state properties.

For the spin-isospin channel, we use the Nakayama interaction which is based on detailed G-Matrix calculations [13]. The $S = 1, T = 0$ force is poorly known, but it is expected to be small. Furthermore the relative contribution in (p,p') scattering is also small. For these reasons we simply approximate this response by the mean-field response, i. e. $v_{S=1,T=0} = 0$.

One last remark is in order here: it is well-known that the RPA response can become unstable at low densities and low energy and momentum transfers, i. e. it can develop an imaginary root. A numerical check showed, however, that this problem occurs only at very low densities, which means at large values of R. Here the free response function Π^{0TF} in the numerator of equation (3) becomes very small. In addition, we have to integrate over all values of R, and so the error due to this instability is never larger than some few per cent.

3. Surface Response Calculation.

The surface response of semi-infinite nuclear matter is described in detail in ref. [1]. Application

to inelastic scattering with the eikonel approximation for the projectile wave function follows the treatment of ref. [14]. A survey of quasi-elestic (p,p') scattering over the energy range $300 - 800$ MeV was made in ref. [15]. The energy and target dependences of the quasi-elastic peak are quite accurately described by the model for momentum tranfers ≥ 250 MeV/c.

The basic formula for the differential inelastic scattering cross section is

$$\frac{d\sigma}{d\omega dE} = \frac{N_{eff}}{S_{norm}} \sum_i \left(\frac{d\sigma}{d\omega}\right)^{el}_{i,\theta,E_p} S_i(q,\omega), \tag{7}$$

where S_i is a strength function for the surface response. The finite nuclear geometry affects the cross section mainly through the prefactor, N_{eff}/S_{norm}. The strength function is calculated from the RPA polarization operator as

$$S_i(q,\omega) = \frac{-1}{\pi} \int_0^{2\pi} d\theta \int dz dz' F(z) F^*(z') e^{iq\,cos\theta(z-z')} \Pi_i^{SR-RPA}(z,z',qsin\theta,\omega), \tag{8}$$

where $qcos\theta$ is the momentum transfer perpendicular to the surface and $qsin\theta$ is parallel to the surface.

The RPA polarization operator is related to the free one by an equation similar to eq. (3). The latter is given by

$$\Pi^{0SR}(z,z',q_x,\omega) =$$

$$\sum_{p,h}{}' \phi_p(z)\phi_h(z)\phi_p^*(z')\phi_h^*(z')\left(\frac{1}{\epsilon_p - \epsilon_h - \omega - i\eta} + \frac{1}{\epsilon_p - \epsilon_h + \omega + i\eta}\right) \tag{9}$$

The $\phi_{p,h}$ are particle and hole wave functions for seminfinite nuclear matter with the surface at $z = 0$. The summation is restricted to states in which the difference in the component

of momentum parallel to the surface is given by q_x. The single particle wave functions are eigenstates of a Woods-Saxon potential, with depth 45 MeV and thickness parameter 0.75 fm. The Fermi energy is taken as 38 MeV, so the separation energy is 7 MeV. The residual interaction is taken to have the separable form, as described in ref. [1].

The projectile form factor is determined from the eikonal χ by the equation

$$F(z) = \sqrt{2\pi(R+z)\chi(z)exp(-\chi(z))/\rho_0(z)} \tag{10}$$

where $\rho_0(z)$ is the nuclear density. For further details see ref. [14]. Besides the nonlocality, eq. (8) includes the diffractive effects of the projectile absorption on the target. This is essentially controlled by the rate of change of the profile function, $exp(-\chi(z))$.

The overall normalization of the cross section is controlled by two factors, N_{eff} and S_{norm}. These factors are defined to give the cross section and response in the limit where the target nucleons scatter completely independently. For the single nucleon scattering cross section we have

$$N_{eff} = \int d^2b \frac{\chi}{\sigma} exp(-\chi) \tag{11}$$

The cross section in this formula should be the effective nucleon-nucleon cross section that produces inelastic scattering. We use a cross section of 25 mb at 290 MeV, 27 mb at 400 MeV, and 30 mb at 500 MeV. These are slightly below the free NN cross section, for reasons discussed in ref. [15]. For the case studied below, proton scattering on a ^{208}Pb target, N_{eff} has the value 16.2, 14.6, and 12.6, respectively. The response is normalized with

$$S_{norm} = \int dz \rho_0(z) F^2(z) \tag{12}$$

which is the total energy-integrated response one would obtain by neglecting the Pauli blocking

and the effect of RPA correlations.

4. Comparison of Models and Data

Let us come now to the applications of the theoretical formalisms and to the comparison of models and experimental data. As already mentioned above, the main differences between the two models will reflect the use of different residual interactions.

In ref. [3,4] data are given for ^{208}Pb(p,p') at energies ranging from 290 to 500 MeV. Comparisons to the data at 290 MeV are are shown in Fig. 1. At moderate momentum transfers, q between $100 - 200$ MeV/c, both models describe the data rather well, both in magnitude and shape. Compared to the independent particle model, the inelastic cross section is enhanced at low excitation energies and this is reproduced by the RPA treatment.

At the highest momentum transfer, q $\sim$ 400 MeV/c, both models, but particularly the Thomas-Fermi model, predict more concentration of strength in the quasi-elastic peak than the data shows.

At the lowest momentum transfer, q $\sim$ 80 MeV/c, both models underpredict the data. The energy integrated cross section is roughly $2/3$ of the measured cross section for the surface response model, and $1/2$ of the cross section for the Thomas-Fermi model. The shape of the energy distribution is roughly correct for the surface response model but it is too skewed to low energies for the Thomas-Fermi model. One must, however, remember that at such small momentum transfers the Thomas-Fermi model is on its edge of validity [2]. Both models miss the low-lying states and the giant resonances, as expected, since they are finite size effects.

Comparisons to the data at 400 MeV are shown in Fig. 2. At the lowest momentum transfer, q $\sim$ 100 MeV/c, both models underpredict data somewhat. The shapes look reasonable except, of course, for the giant resonances. At higher momentum transfers the Thomas-Fermi model gives too large a cross section while the surface response model is too low. Again the shape looks quite reasonable.

The analysis of the 500 MeV case in Fig. 5 shows that both models do quite well at the lowest momentum transfer at $\theta_L = 5$ °. Going to higher momentum transfers both models overpredict the data with the Thomas Fermi results the poorer of the two. The highest momentum transfer at $\theta_L = 25$ ° deserves some comment. We know from experience that the free surface response gives the quasi-elastic peak position quite accurately at larger momentum transfers[15]. This is also clearly confirmed by the 290 MeV data (see Fig. 4 of Ref. [4]). In the present case (25 ° at 500 MeV) the theoretical and experimental peak positions are off by more than 30 percent. This could indicate some difficulties with the experimental data. On the other hand, the residual interaction used in the Thomas Fermi model does not seem to fall off fast enough as the momentum transfer increases, causing the strong peak in the $\theta_L = 25$ ° results.

5. Conclusions

In this paper, we confronted the surface response model, the Thomas-Fermi model and the data for quasi-elastic (p,p') scattering on lead. Both models describe the data within a factor of two or better in the momentum range $100 - 400$ MeV/c and outside the spectroscopic domain. In the region of low lying collective states, however, the models describe the situation roughly on the average. On the other hand, there may be some experimental difficulties in the 500 MeV data at the largest measured scattering angle.

At the lowest momentum transfers considered here (100 MeV/c), the surface response model is somewhat superior, both absolute magnitude and in shape. This is to be expected since the Thomas-Fermi model is more reliable at the higher q values. Otherwise, both models agree quite well inspite of their somewhat different ingredients. Indeed, whereas the surface response model uses a separable force of the Bohr-Mottelson type, the Thomas- Fermi model uses the finite range Gogny force with anti- symmetrization effects included. This is possible in the Thomas-Fermi model, because it is numerically less involved.

The underprediction of the cross section at the smallest momentum transfers and lowest projectile energy may be a result of wave distortion effects from the central potential, which are neglected. It might also be due in part to the contribution of two-step reactions, which become

important at low beam energy and high excitation energy [15].

The fact that the quasi-elastic peak at high momentum transfers is broader than predicted may show an intrinsic limitation of RPA. Other interactions not included in RPA are expected to broaden the peaks.

Acknowledgement:

One of the authors (J.J.) would like to thank J. Peters for the help to perform the figures. This work was supported (G.B. and H.E.) by the National Science Foundation under grant PHY 87-14432 (G.B. and H.E.). One of us (H.E.) is also supported by the U.S Department of Energy, Nuclear Physics Division under contract W-31-109-ENG-38 and another one (J.J.) by the German Federal Ministry for Research and Technology (BMFT) under the contract numbe 06 HD 710 and by the Gesellschaft für Scherionenforschung (GSI) under contract number HD HU T.

Figure captions:

Figure 1: The differential cross section of quasi-elastic proton scattering on Pb at 290 MeV and different scattering angles. The experimental data are taken from ref. [3,4]. The heavy solid line corresponds to the Thomas Fermi model calculation, the dashed line to the surface response model results and the thin solid line gives the free response result.

Figure 2: Same as fig. 1 but for the energy of 400 MeV.

Figure 3: Same as fig. 1 but for the energy of 500 MeV.

References:

[1] H. Esbensen and G. Bertsch, Ann. Phys. 157 (1984) 255.

[2] P. Schuck, R.W. Hasse, J. Jaenicke, C. Grégoire, B. Rémaud, F. Sébille and E. Suraud, Prog. Part. Nucl. Phys. 22 (1989) 181.

[3] X.Y. Chen et al., Phys. Lett. 205B (1988) 436.

[4] X.Y. Chen et al., Nucl. Phys. A505 (1989) 670.

[5] G. Chanfray and P. Schuck, Phys. Rev. A38 (1988) 4832.

[6] T. Izumoto, M. Ichimura, C.M. Ko and P.J. Siemens, Phys. Lett B112 (1982) 315.

[7] S.J. Wallace, Adv. in Nucl. Phys. 12 (1981) 135.

[8] U. Stroth R.W. Hasse, P. Schuck, W.M. Alberico, M. Ericson and A. Molinari, Phys. Lett. B156 (1985) 291.

[9] J. Dechargé and D. Gogny, Phys. Rev. C21 (1980) 1568.

[10] J. Jaenicke, P. Schuck and R.W. Hasse, Phys. Lett. B214 (1988) 1.

[11] P. Schuck, J. Low Temp. Phys. 7 (1972) 459.

[12] U. Stroth, R.W.Hasse and P. Schuck, Nucl. Phys. A462 (1987) 45.

[13] K. Nakayama, S. Krewald, J. Speth and W.G. Love, Nucl. Phys. A431 (1984) 419.

[14] H. Esbensen, H. Toki, and G. Bertsch, Phys. Rev. C31 (1985) 1816.

[15] H. Esbensen and G. Bertsch, Phys. Rev. C32 (1985) 553.

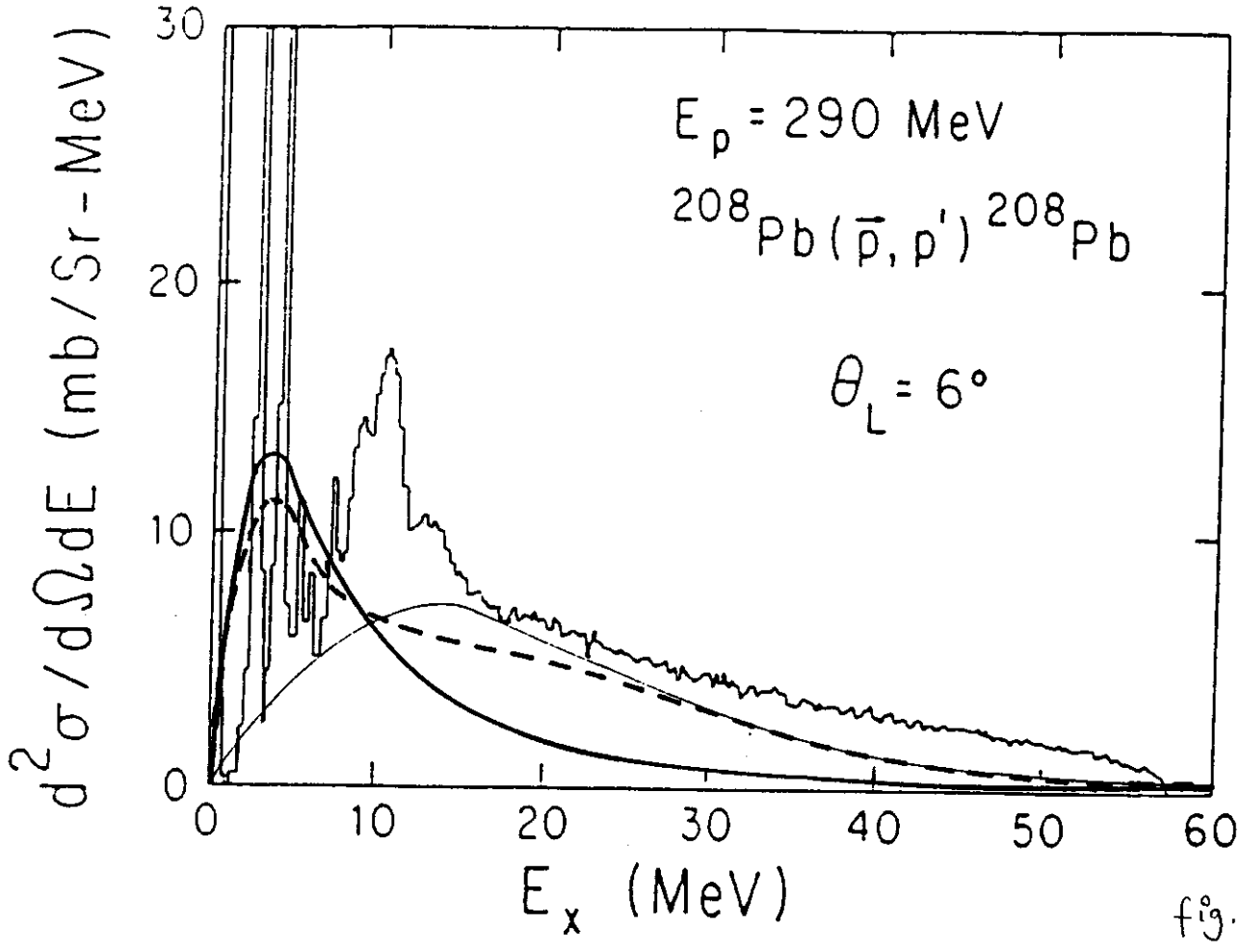
E_p = 290 MeV
$^{208}Pb(\vec{p},p')^{208}Pb$
θ_L = 6°
$d^2\sigma/d\Omega dE$ (mb/Sr-MeV)
E_x (MeV)
0
10
20
30
40
50
60

fig. 1

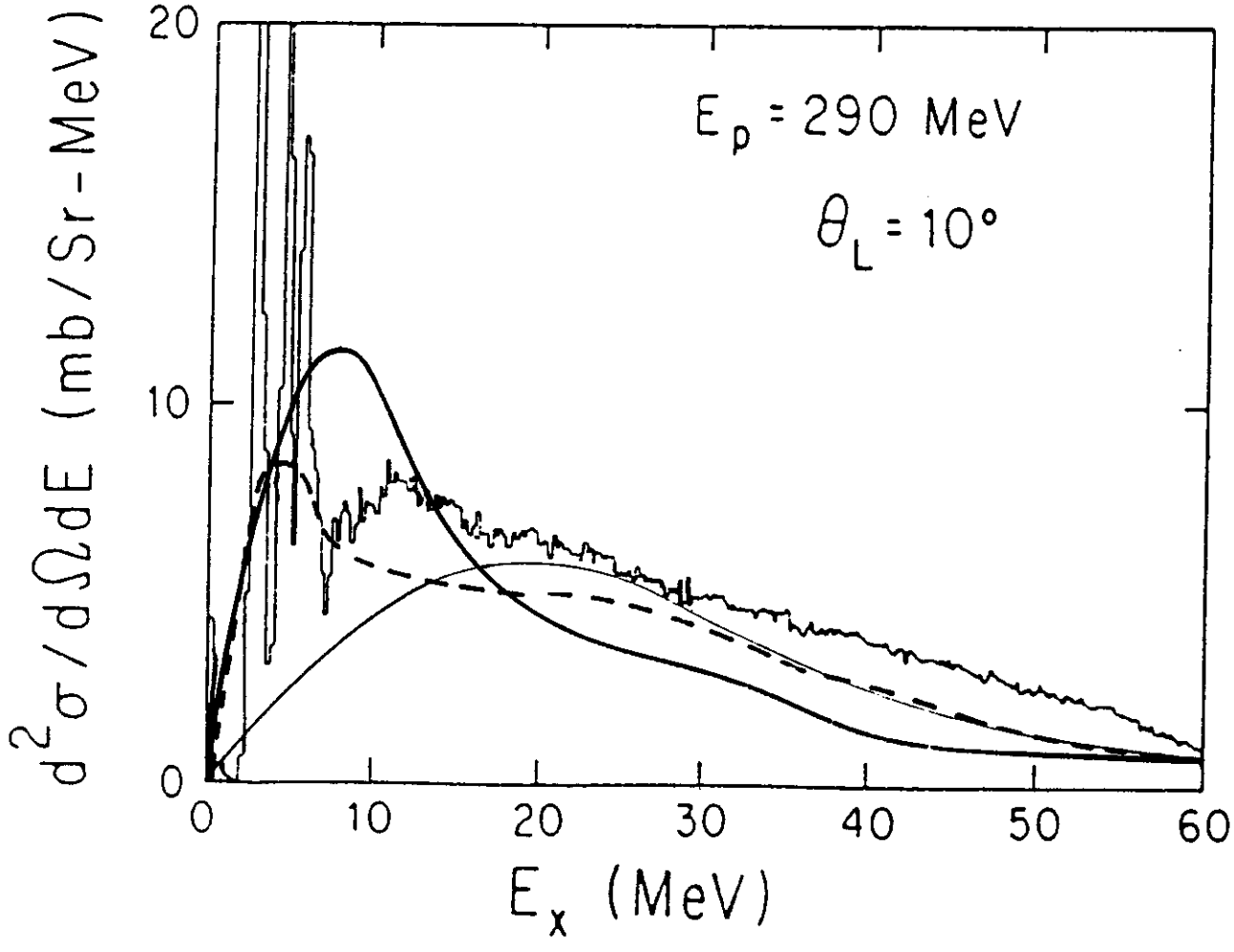
E_p = 290 MeV
θ_L = 10°
$d^2\sigma/d\Omega dE$ (mb/Sr-MeV)
E_x (MeV)
0
10
20
30
40
50
60
0
10
20

fig. 1

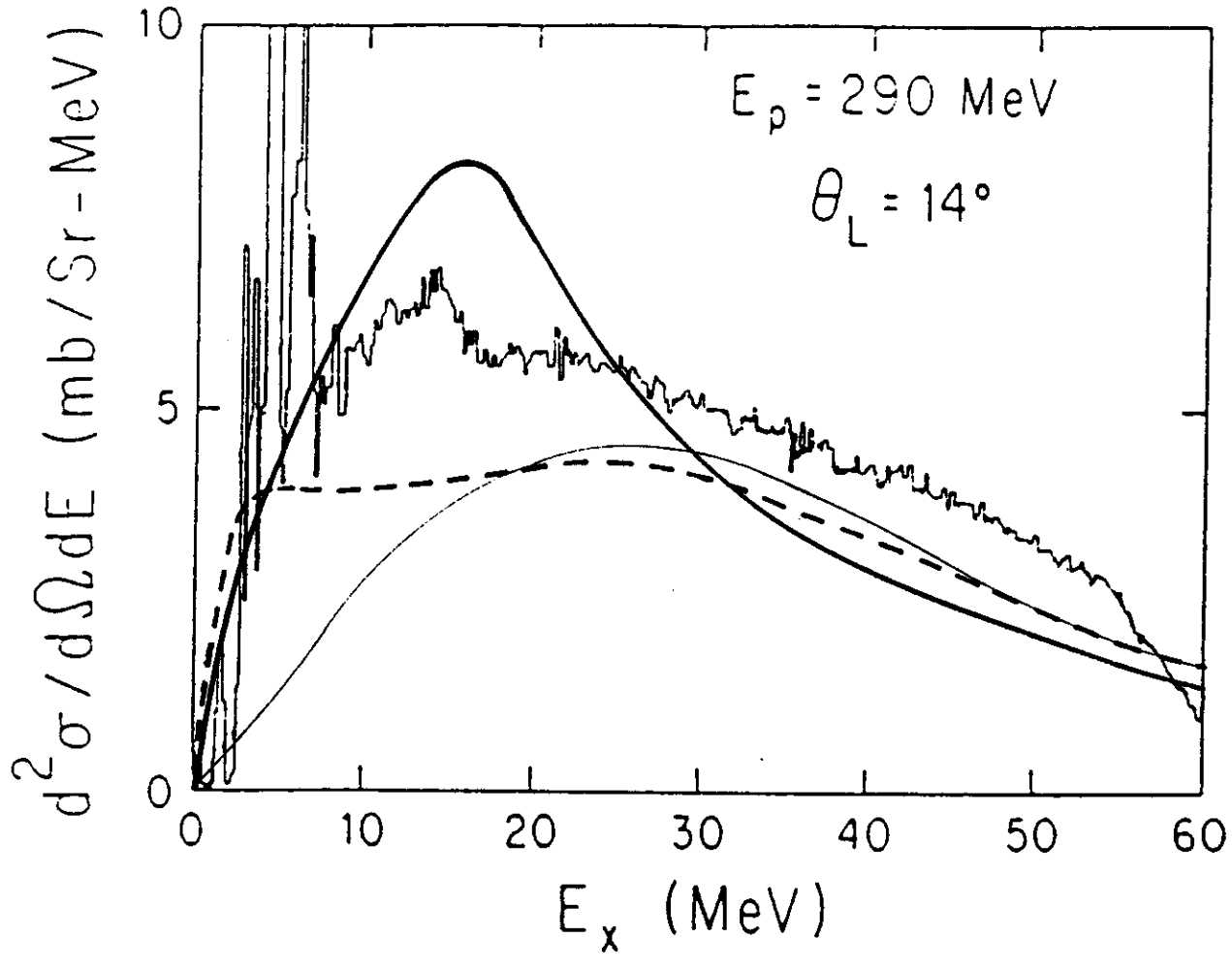
E_p = 290 MeV
θ_L = 14°
$d^2\sigma/d\Omega dE$ (mb/Sr-MeV)
E_x (MeV)
0
5
10
0
10
20
30
40
50
60

fig. 1

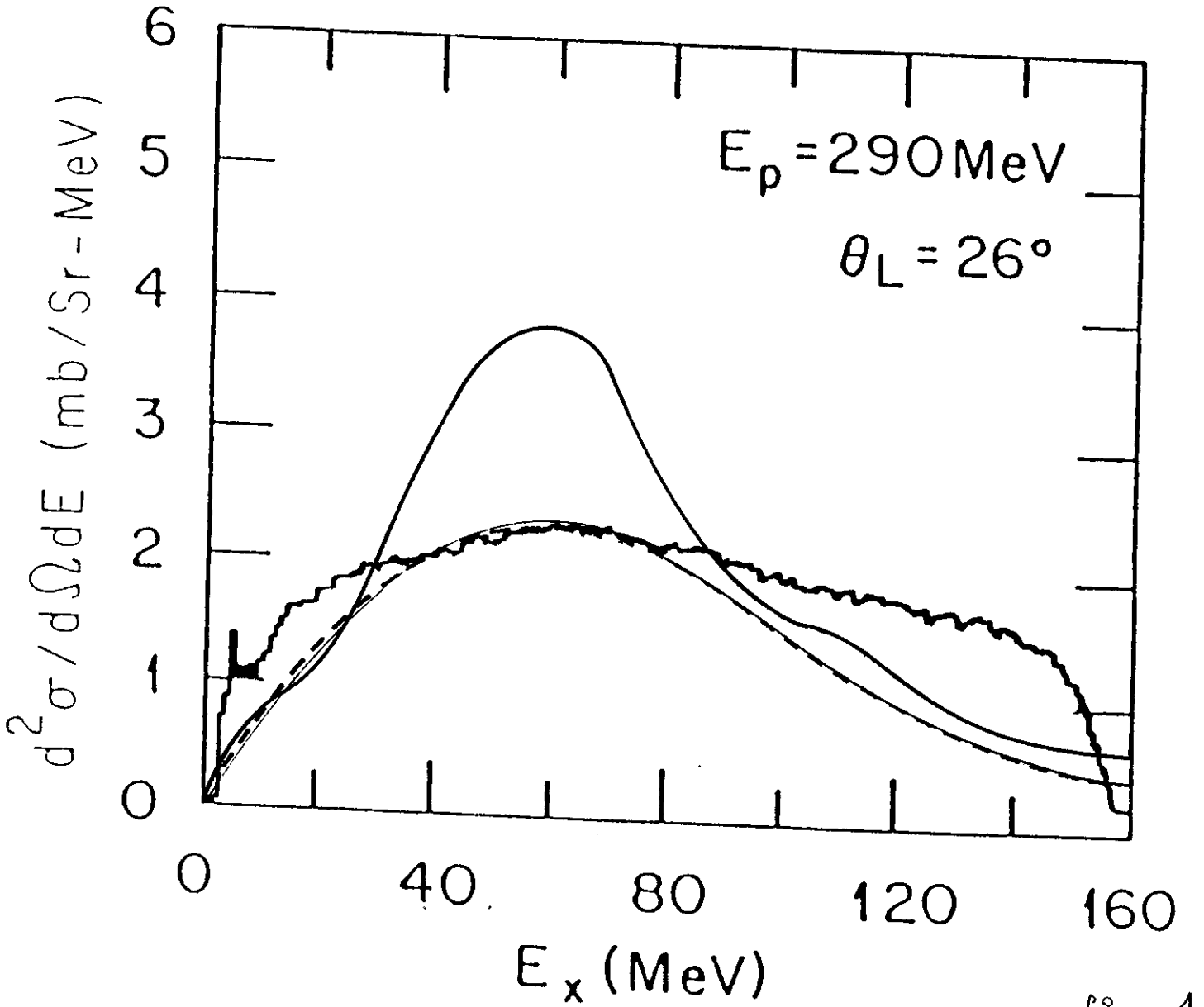
$E_p = 290\,MeV$
$\theta_L = 26°$
$d^2\sigma/d\Omega dE$ (mb/Sr-MeV)
E_x (MeV)
0
1
2
3
4
5
6
0
40
80
120
160

fig. 1

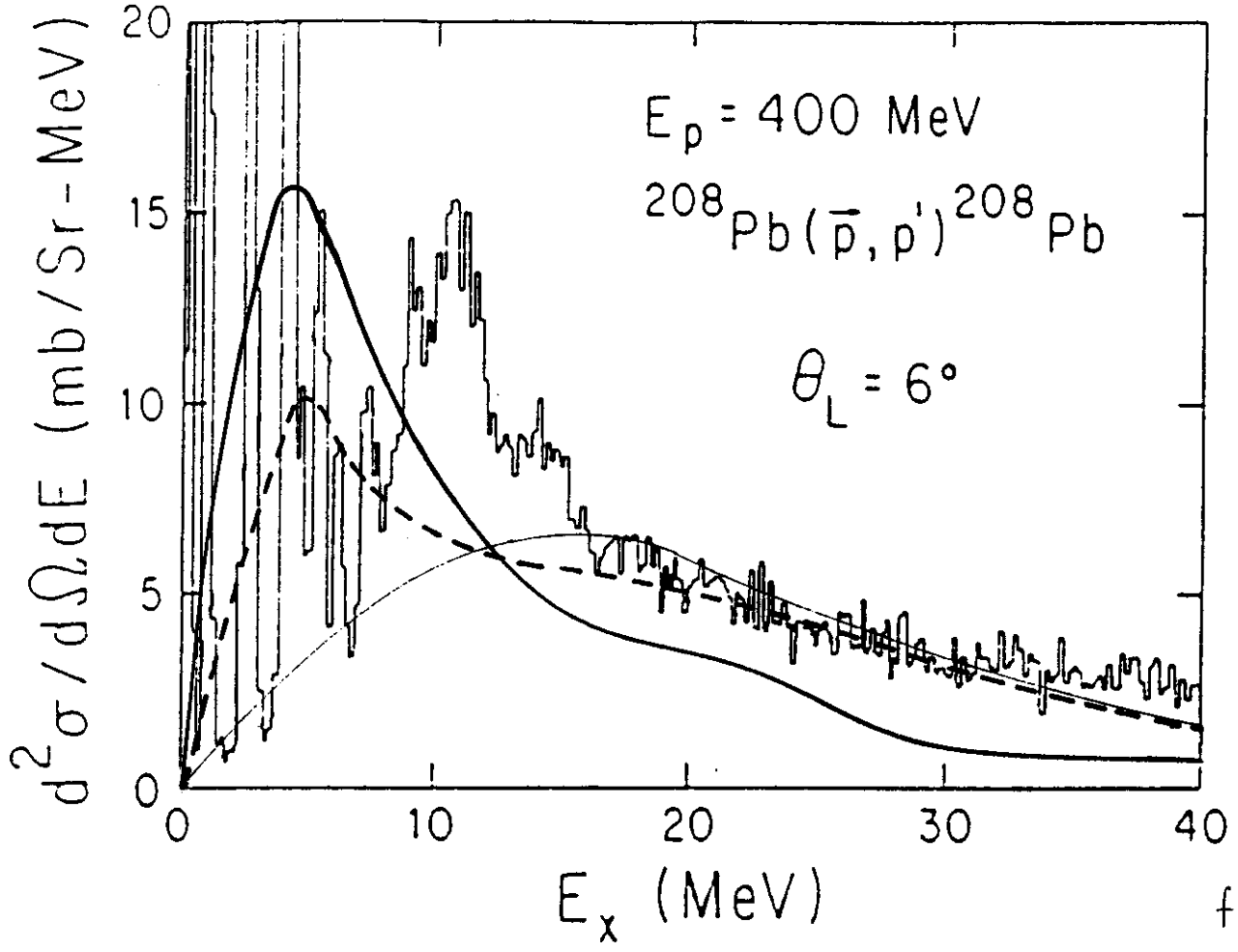
E_p = 400 MeV
$^{208}Pb(\vec{p},p')^{208}Pb$
θ_L = 6°
$d^2\sigma/d\Omega dE$ (mb/Sr-MeV)
E_x (MeV)
0
5
10
15
20
0
10
20
30
40

fig. 2

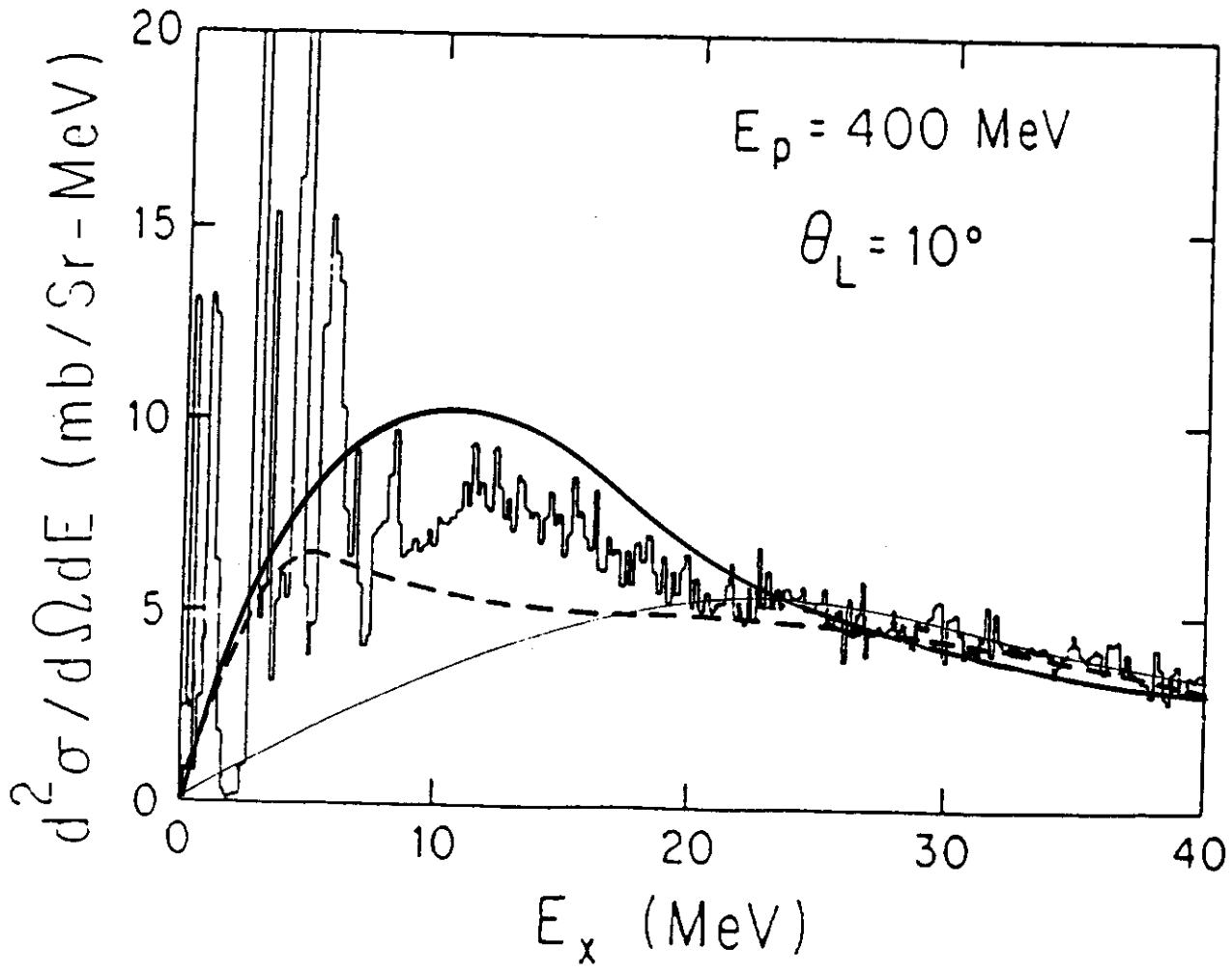
E_p = 400 MeV
θ_L = 10°
$d^2\sigma/d\Omega dE$ (mb/Sr-MeV)
E_x (MeV)
0
5
10
15
20
0
10
20
30
40

fig. 2

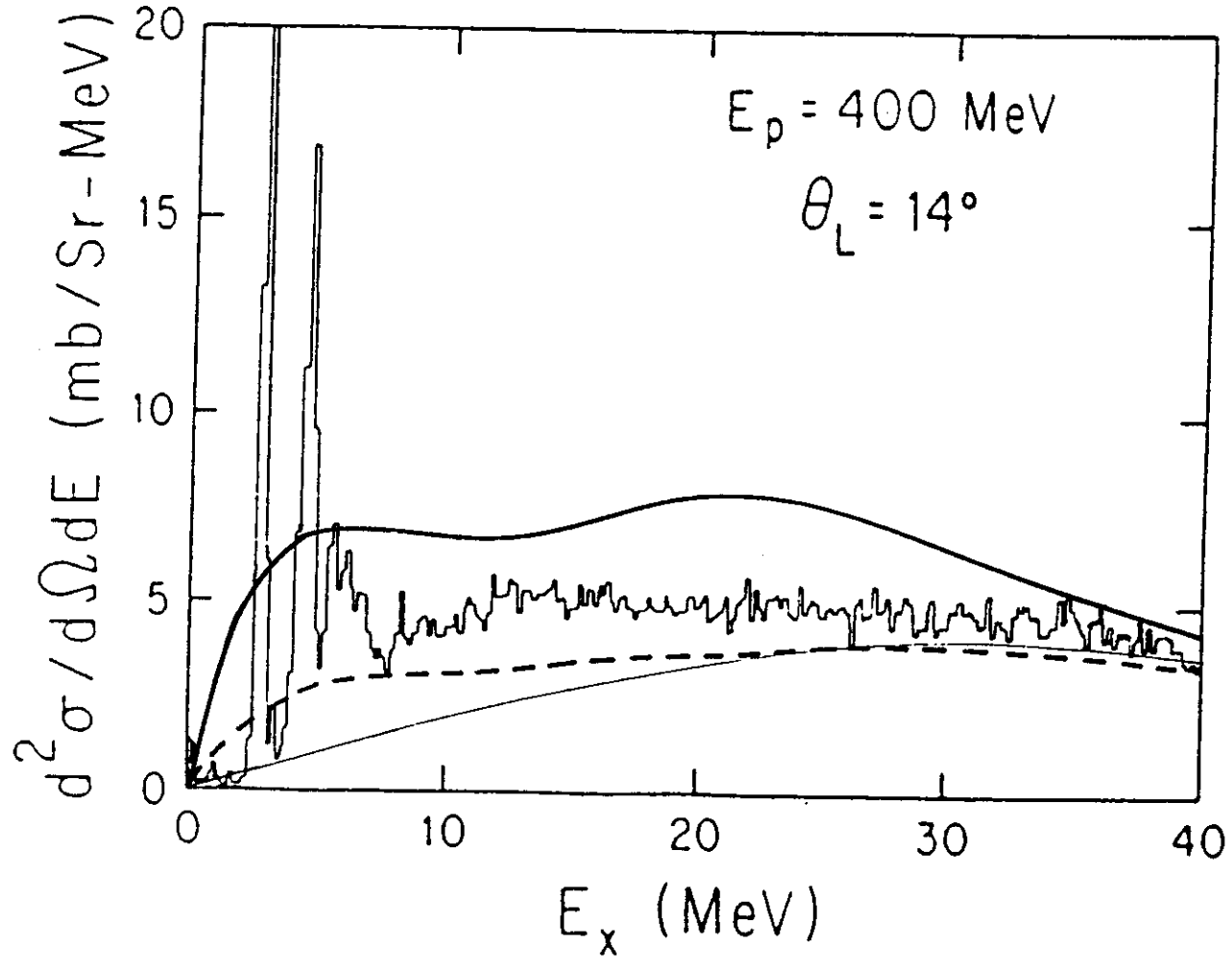
E_p = 400 MeV
θ_L = 14°
$d^2\sigma/d\Omega dE$ (mb/Sr-MeV)
E_x (MeV)
0
5
10
15
20
0
10
20
30
40

fig. 2

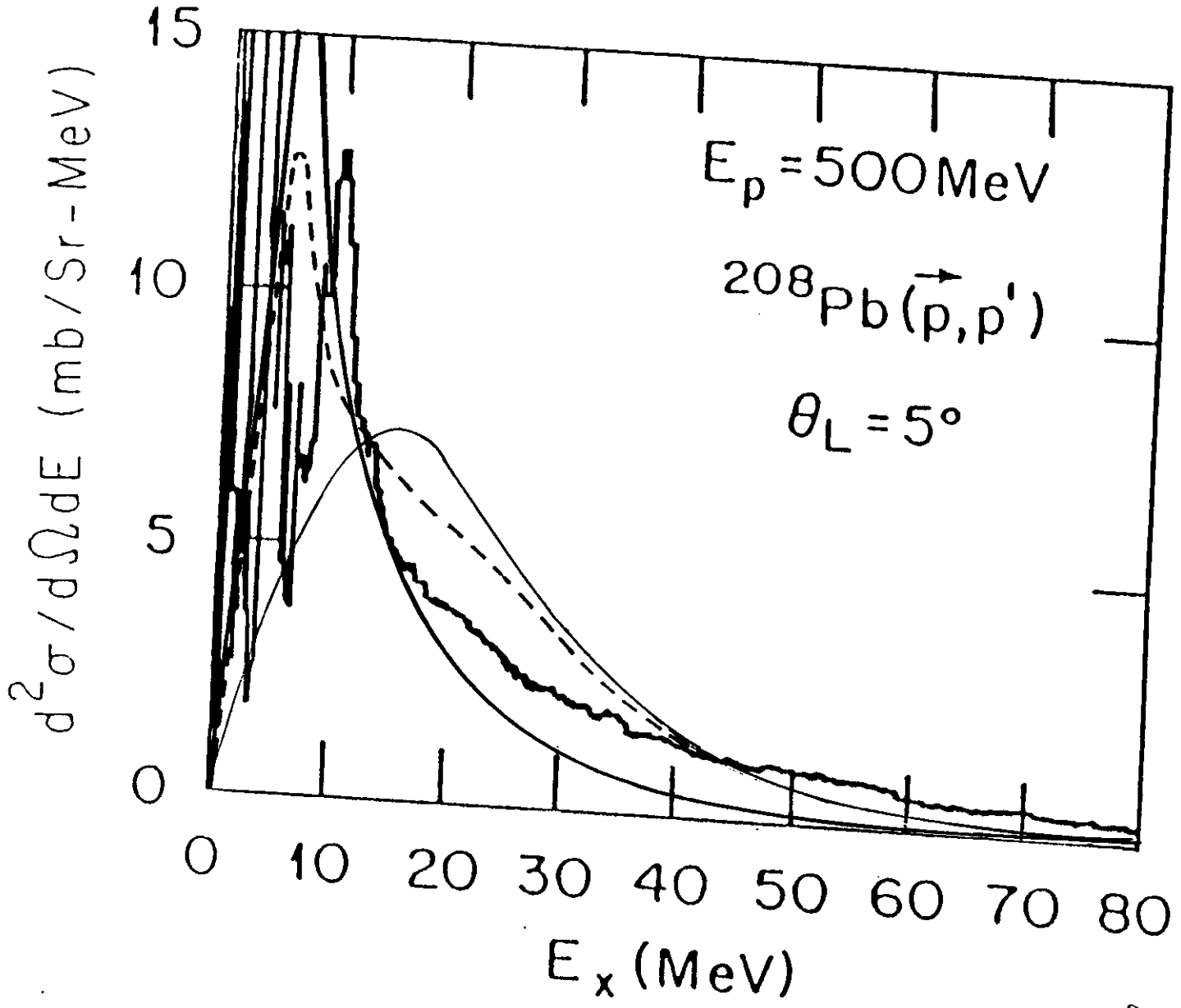
15
10
5
0
$d^2\sigma/d\Omega dE$ (mb/Sr-MeV)
$E_p = 500$ MeV
$^{208}Pb(\vec{p},p')$
$\theta_L = 5°$
0 10 20 30 40 50 60 70 80
E_x (MeV)

fig. 3

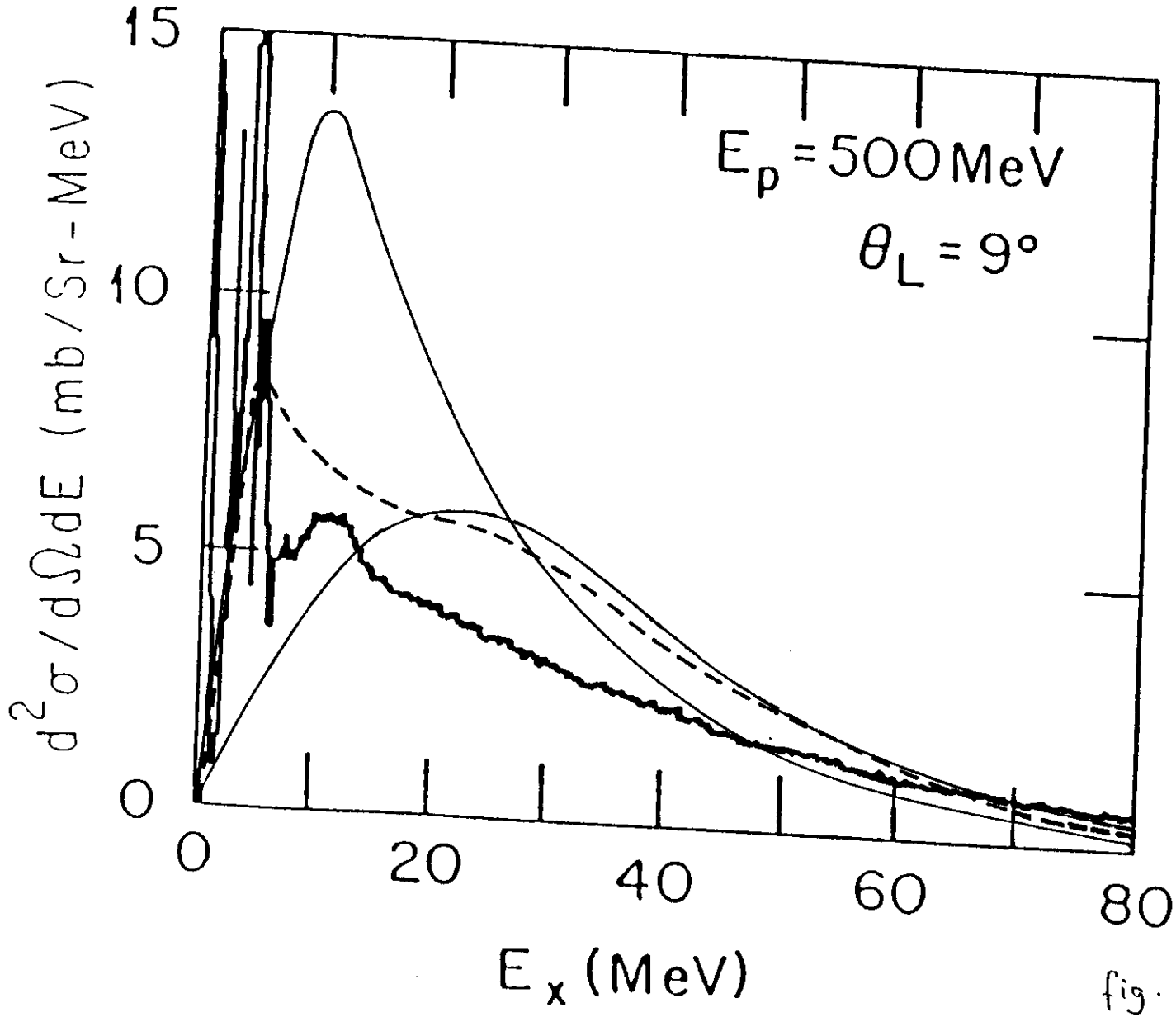
15
10
5
0
0
20
40
60
80
$E_p = 500\,MeV$
$\theta_L = 9°$
$d^2\sigma/d\Omega dE$ (mb/Sr-MeV)
E_x (MeV)

fig. 3

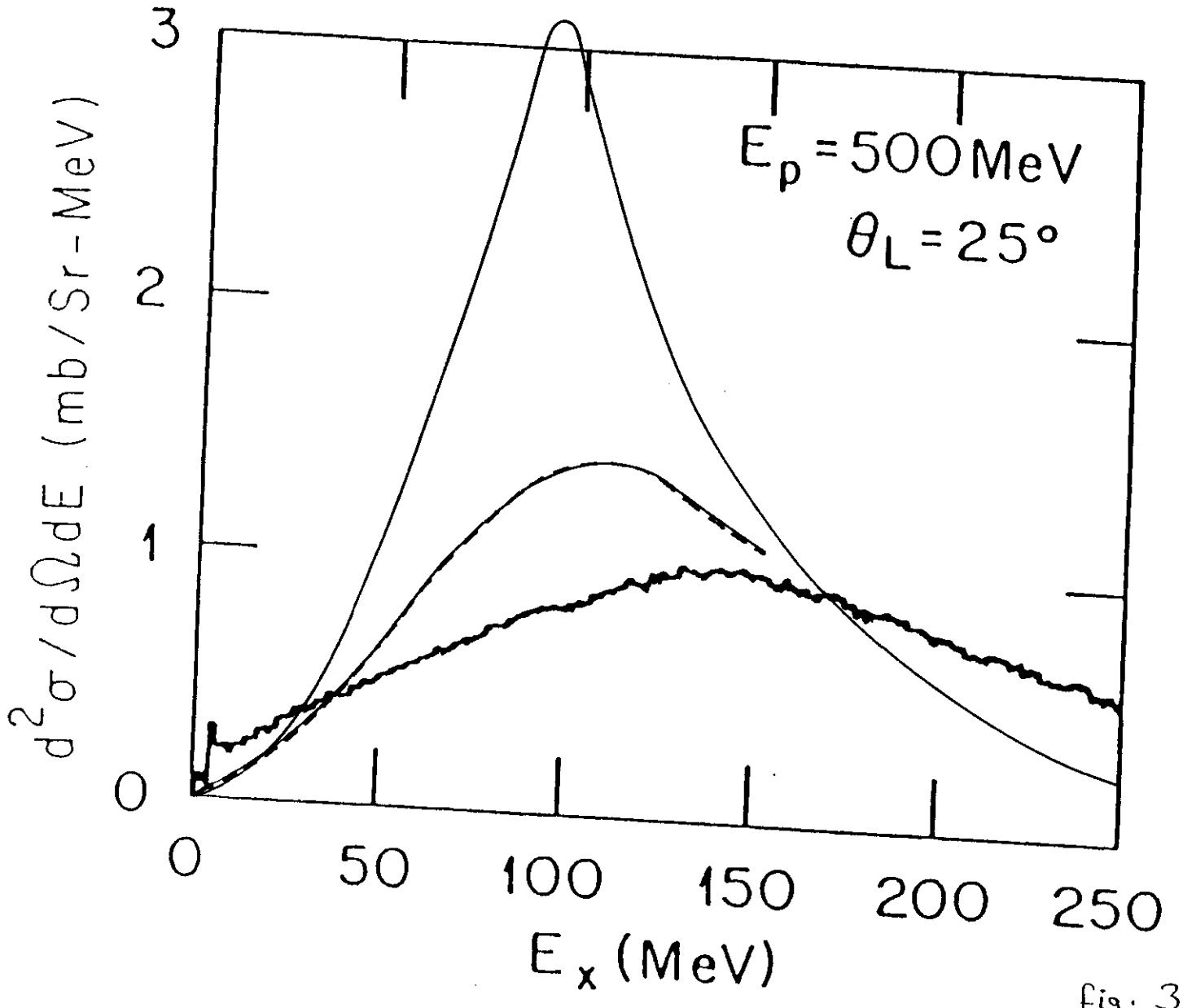
$E_p = 500\,MeV$
$\theta_L = 25°$
$d^2\sigma/d\Omega dE$ (mb/Sr-MeV)
E_x (MeV)
0
1
2
3
0
50
100
150
200
250

fig. 3